Corrosion of Target and Structural Materials in Water Irradiated by an 800 MeV Proton Beam

Darryl P. Butt, Gary S. Kanner, and R. Scott Lillard
Materials Science and Technology Division
Los Alamos National Laboratory
Los Alamos, NM 87545 U.S.A.

Abstract

Radiation enhanced, aqueous corrosion of solid neutron-targets such as tungsten or tantalum, or target cladding or structural materials such as superalloys and stainless steels, is a significant concern in accelerator-driven transmutation technologies. In this paper we briefly describe our current methods for control and *in situ* monitoring of corrosion in accelerator cooling water loops. Using floating, electrochemical impedance spectroscopy (EIS), we have measured the corrosion rates of aluminum 6061, copper, Inconel 718, and 304L stainless steel in the flow loop of a water target irradiated by a μamp, 800 MeV proton beam. Impedance spectroscopy allows us to model the corrosion process of a material as an equivalent electrical circuit. Thus the polarization resistance, which is inversely proportional to the corrosion rate, can be extracted from the frequency response of a metal specimen. During a three month period, without the use of corrosion mitigation techniques, we observed increases of several orders of magnitude in the water conductivity and the corrosion rates. The increase in corrosion is at least partially attributed to a build up of peroxide in our pseudo-closed loop system.

In this paper we also briefly describe our second generation experiments, scheduled to begin in late 1996. In these experiments we plan to measure the corrosion rates of tungsten, tantalum, Inconel 718, 316L and 304L stainless steel, HT-9 austenitic stainless steel, and aluminum 5053. Two or three electrode probes of each material are being placed directly in the proton beam, in a high neutron flux region, or a significant distance from the high radiation area. We will be measuring corrosion rates, changes in pH and conductivity, and we will be establishing parameters for filtration and mitigation of corrosion. We will also discuss our ideas for making *in situ* measurements of water radiolysis using optical and laser diagnostic techniques. Using such techniques it is possible to directly observe the production of corrosive radiolysis products as well as corrosion products near the surface of a target in a high energy particle beam.

Introduction

It is well known, primarily from the wealth of experience with nuclear reactors, that radiation can significantly accelerate the aqueous corrosion of materials.[1] In a radiation environment, elementary particles passing through water will lead to its radiolysis as follows:

$$H_2O \rightarrow OH, H, H_2, H_2O^+, H_2O_2, e_{aq}, ... \quad (1)$$

The majority of radiolysis products, or radicals, have lifetimes of milliseconds or less. The concentrations of some species, H_2O_2 in particular, can build up to relatively high steady state concentrations. Both short lived and long lived radicals can lead to accelerated corrosion. In an accelerator environment, the short lived radicals are primarily a concern only when produced very near a metal surface, that is, a surface directly impinged by the high energy particle beam. As the beam travels through and radiolyzes water, it can produce concentrations of radicals along its track of the order 1-3 M.[1] The concentration of these species becomes vanishingly small just a short distance away.

In addition to radiolysis products, radiation damage can affect the corrosion behavior of a material. In particular, elastic collisions between the incident, high energy particles and the nuclei of the material leads to large local atomic displacements which result in irreversible plastic deformation and heating. Generally this produces a material with a higher configurational free energy,

which typically leads to more rapid corrosion. However, under certain conditions a higher free energy can lead to the rapid formation of a protective, passive oxide.

Thus, we have set out to develop techniques to both measure and directly observe the corrosion of materials in the radiation environments produced by a high energy particle beam. The techniques we are developing are aimed at understanding the corrosion of materials in or near the path of a high energy beam as well as some distance away where only stable radiolysis products are important. A number of proof-of-concept experiments have been conducted this past year, and will be described below. In addition, we briefly describe a second series of experiments for which are currently preparing that will make use of more sophisticated diagnostics.

Impedance Spectroscopy

Electrochemical Impedance Spectroscopy (EIS) was used to evaluate the corrosion of copper, aluminum 6061, Inconel 718, and 304L stainless steel in a pseudo-closed water loop, irradiated by an 800 MeV particle beam as illustrated schematically in Fig. 1. The particle beam passed through a so called degrader, consisting essentially of a complex network of water channels that served to maximize the time that the water spent in contact with the beam. Thus, the water leaving the degrader was highly radiolyzed. Because the system was pseudo-closed loop (meaning the rate of water added and removed from the system was small compared to the total system volume) it was anticipated that long lived radiolysis products, namely H_2O_2, would build up in the system until a steady state level was achieved. Corrosion cells were plumbed into the degrader loop both on the supply and return sides. The corrosion cells were shielded from direct radiation and were located approximately 5 meters above the degrader and so changes in corrosion were from changes in water chemistry not from radiation damage. Three three-electrode corrosion probes, as illustrated in Fig. 2, were inserted into each corrosion cell. These probes consisted of either one or two samples, or working electrodes, and one or two C-276 reference electrodes.

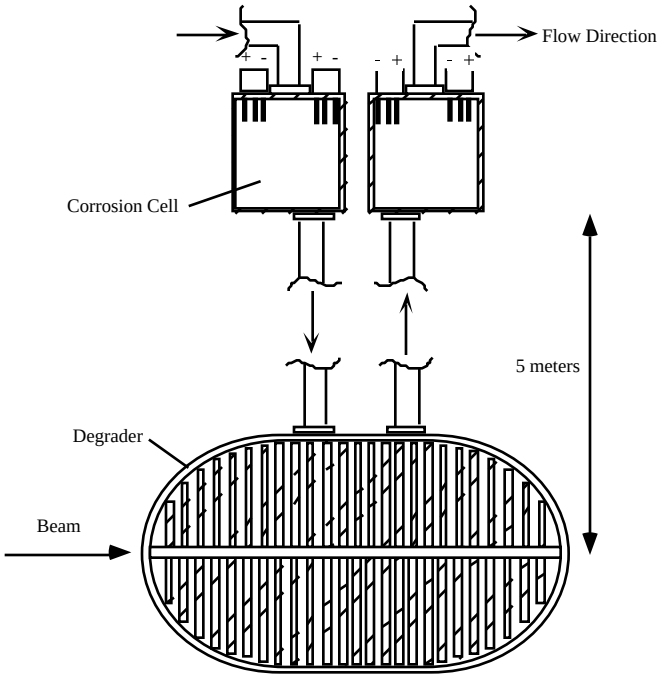

Fig. 1. Schematic illustration of the pseudo-closed loop flow system used to measure the effects of radiolyzed water on corrosion. Not drawn to scale.

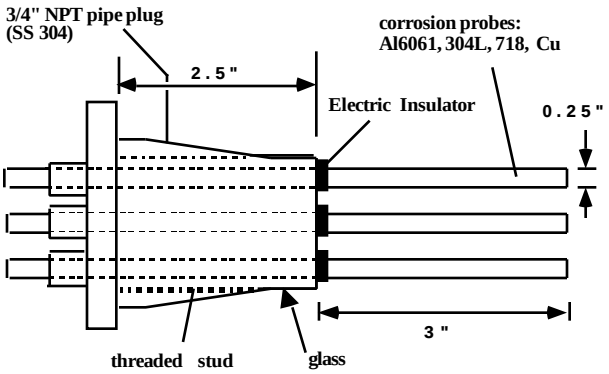

Fig. 2. Schematic illustration of a three-electrode corrosion probe.

Using floating EIS, we measured the time-dependent current response of the electrode surfaces to small sinusoidal, alternating potentials. Thus, by fitting the data to equivalent electric circuit models, we could determine response variables such as corrosion rate (inversely proportional to polarization resistance), and solution conductivity (inversely proportional to geometric solution resistance). Fig. 3 shows an example of measurements made on 304L stainless steel on the return side of the degrader loop. The data are represented in this figure as both Bode magnitude (impedance, Z) and Bode phase (phase shift, θ) plots. The corrosion rates and solution conductivities are thus calculated by determining the equivalent circuit components R_{pol} and R_{sol} shown in Fig. 3.

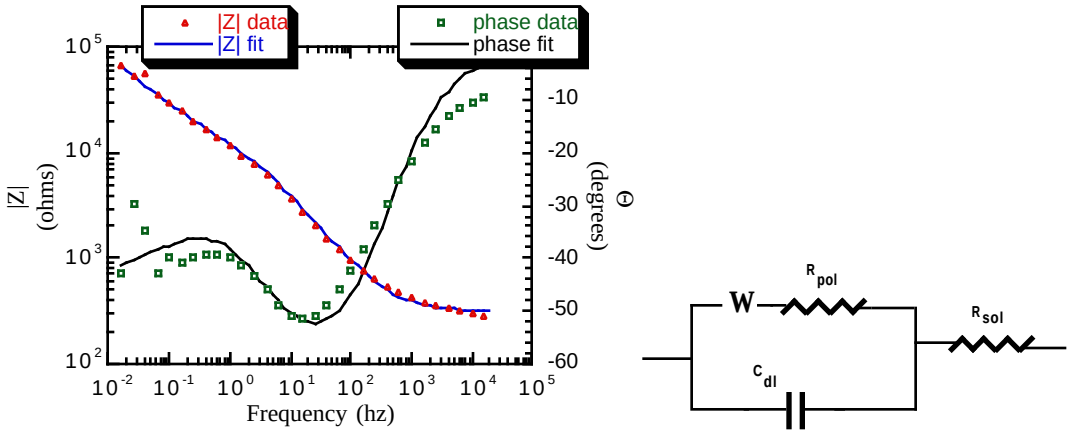

Fig. 3. EIS data and schematic of the corresponding equivalent circuit, obtained during a corrosion measurement taken on 304L stainless steel in a pseudo-closed loop flow system of a water target radiolyzed by an 800 MeV particle beam. W is the Warburg impedance (a diffusion term), R_{pol} is the polarization resistance (inversely proportional to corrosion current), R_{sol} is the solution resistance, C_{dl} is the double layer capacitance.

Equivalent circuit models, such as that illustrated in Fig. 3, were determined for each material in the closed loop system as a function of time. As shown in Figs. 4 and 5 below, during a three month period, without the use of corrosion mitigation techniques, we observed increases of several orders of magnitude in the water conductivity and the corrosion rates. The increase in conductivity is at least partially attributed to a build up of peroxide and metal ions in our pseudo-closed loop system. The corrosion rates increased steadily due to the build up of peroxide, that is, cathodic reactants, which apparently had not reached a steady state level by the end of this series of measurements. It is notable that over the course of two months, the corrosion rates of the four materials increased by one to four orders of magnitude due to the effects of radiolysis. Further details on these and other corrosion measurements have been reported elsewhere.[2]

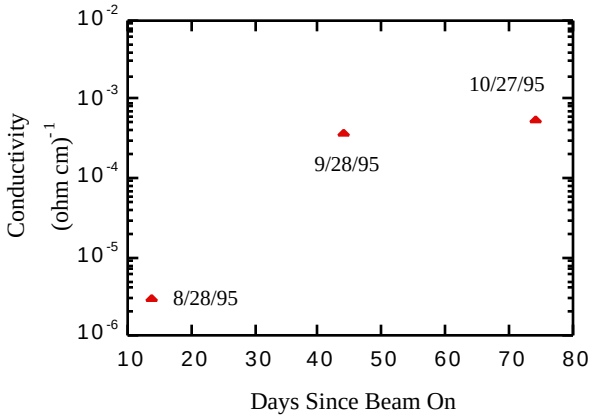

Fig. 4. Chronology of conductivity measurements made by EIS in the water target flow system.

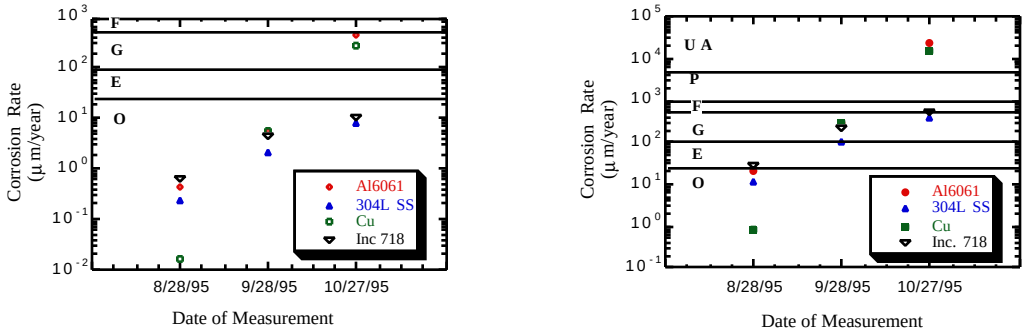

Fig. 5. Chronology of corrosion rates measured by EIS in the water target flow system: (a) shows the rates assuming uniform corrosion, and (b) shows the rates assuming pitting occurred over 2% of the surface area. The symbols O, E, G, F, P, and UA represent regions of corrosion considered to be outstanding, excellent, good, fair, poor, and unacceptable, respectively.

In our second generation experiments we will measure, by EIS, the corrosion rates of tungsten, tantalum, Inconel 718, 316L and 304L stainless steel, HT-9 austenitic stainless steel, and aluminum 5053. We have designed unique corrosion probes that will be placed directly in the high energy particle beam and in a region of high neutron flux. At this date, the probe designs are proprietary so can not be described in detail. However, they consist essentially of hollow, ceramic sealed tubes instrumented with internal thermocouples. Probes similar to that shown in Fig. 2 will be placed approximately 5 meters above the particle beam, as was done in the degrader loop experiments. In addition to measuring the corrosion rates and water conductivity, we will also monitor pH at several locations in the system using tungsten/tungsten oxide sensing electrodes which exhibit a Nernstian pH response.[3] In the course of these experiments we will also investigate the effects of scavengers, hydrogen in particular, on corrosion. It is well known, primarily from nuclear reactor experience, that hydrogen prevents the recombination of OH into H_2O_2, and thus reduces the levels of cathodic reactant.

In Situ Diagnostics of Corrosion Products

We currently use a machinable tungsten target in our accelerator at Los Alamos. Pure tungsten is also a candidate target for accelerator production of tritium. Therefore, we are particularly concerned with the interaction of tungsten with water radiolysis products. In addition to the *in situ* corrosion measurements described above, we are working toward directly observing the interactions between tungsten and both short and long lived radiolysis products. Towards this end we are developing laser diagnostic methods that will allow us to identify a variety of reactant and product species in a high

energy radiation environment. Currently, we are assimilating base line data for measuring the transient Raman spectra associated with reactive species generated by a high energy proton beam. For example, we have developed laser diagnostics that allow us to directly observe and, thus, correlate the decay of peroxide with the corrosion of tungsten as described below.

We have performed steady state Raman measurements on a tungsten plate immersed in dilute aqueous solutions of H_2O_2 to study the effect of long-lived radiolysis products on corrosion. Before immersion, no Raman modes could be detected from the W surface. As shown in Fig. 6, after immersion, we observe spectral features in the solution that can be attributed to tungsten oxide vibrations.[4-6] As these modes develop, the intensity of the O-O stretch (875 cm^{-1}) of H_2O_2 decreases, suggesting chemical reduction of H_2O_2 and the corresponding corrosion of tungsten. As shown in Fig. 7, this observation is in agreement with dc spectroscopy studies that we have performed on tungsten which demonstrate that the corrosion rate increases with increasing concentrations of cathodic reactant, i.e., H_2O_2. At the initial pH (4±0.5), W is expected to form a passive oxide. Tungsten oxide ions or hydrates may also appear in solution, particularly under alkaline conditions.[7] The tungsten oxide vibrational modes shown in Fig. 6 are associated with terminal W=O or W-O stretches of hydrated oxide molecules. These stretches are observed only in the solution and not on the tungsten surface. Thus, the tungsten is corroding by a dissolution mechanism.

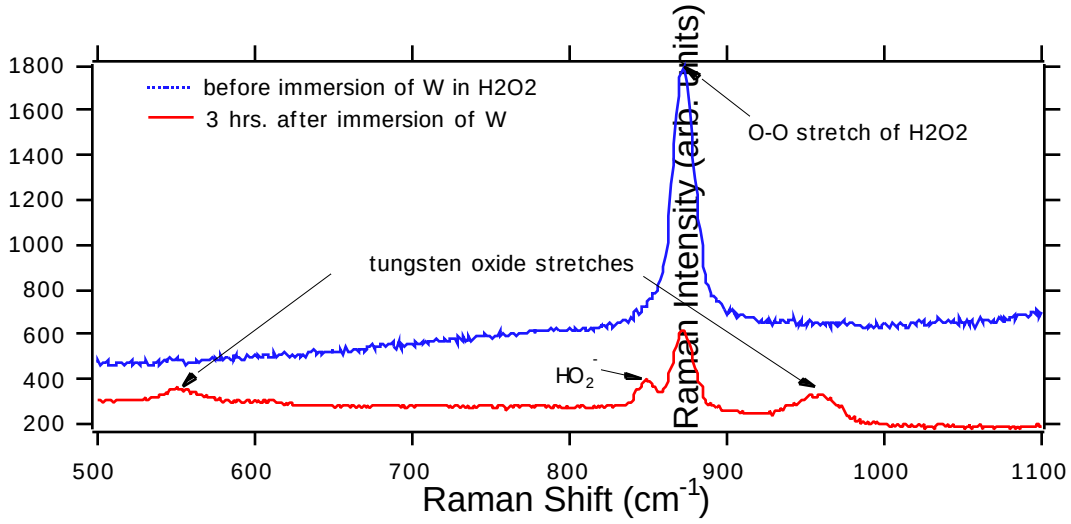

Fig. 6. Steady state measurement of corrosion of tungsten by hydrogen peroxide.

Another interesting result is the appearance of a mode associated with the O-O stretch of HO_2^-. For acidic pH the decomposition of H_2O_2 should give rise to O_2, H_2, or H_2O. However, after immersing W in the solution we observe the formation of a peak at 849 cm^{-1}. We have verified that this peak is due to the peroxide ion by observing a shift of the O-O stretch frequency from 875 to 849 cm^{-1} as the pH of the peroxide solution is changed from 4 to 13, where only the peroxide ion is stable. The HO_2^- peak disappears after 20 hours of immersion of tungsten, decomposing into O_2 and H^+.

The above results were obtained under nonresonant conditions (514.5 nm excitation), and with an instrument optimized for near infrared rather than visible detection. We will repeat the measurements with resonant excitation, and UV-sensitive instruments, in an effort to detect even smaller concentrations of reactive species and products. This will allow us to define the detection limits for each species for our laser system.

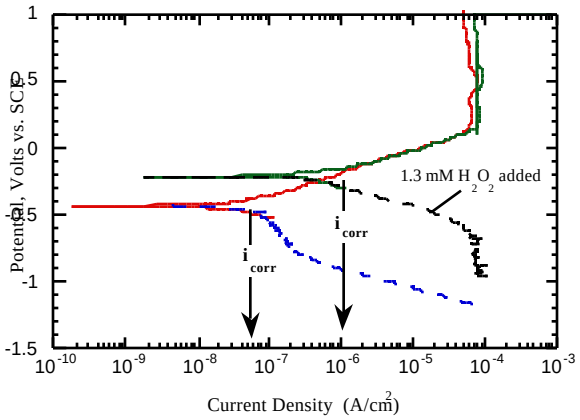

Fig. 7. Polarization curves for tungsten in 0.1 M NaCl, with and without the addition of peroxide. The corrosion rate (proportional to i_{corr}) increases with increased cathodic reactant.

We are currently in the process of preparing for *in situ* laser diagnostic measurements of tungsten to be done using two radiation sources. Later this summer, we will study the radiolysis and corrosion products produced by a free electron accelerator with 10-20 MeV electrons (tunable), 10 Hz (100 ms between pulses), and an electric charge of 2 pC per pulse. In late Fall, we will perform similar studies in a proton beam at 800 MeV, 1 μpulse per macropulse, at 100 Hz (10 ms between pulses). In this way we will be able to study the tungsten/radiolysis interactions under two conditions of highly different linear energy transfer (LET) from particle to media, that is, different levels of energy loss to the medium per unit distance traveled. The free electron accelerator emulates low LET protons while the proton beam simulates a spallation radiation environment. In these experiments, we hope to directly measure G-values, observe radiolytic species and their interactions with tungsten, and observe the effect of scavengers, such as hydrogen, on the surface chemistry.

Acknowledgments

The authors are grateful for the assistance and advice of Ms. Doris Ford, Drs. Walt Sommer, Robert Brown, Robert Jones, Luke Daemen, and Stuart Maloy of Los Alamos National Laboratory, and Dr. Jay LaVerne of University of Notre Dame. This research was funded by the U.S. Department of Energy.

References

1. A. V. Byalobzheskii, *Radiation Corrosion*, TT 70-50005, AEC-tr 7096, U.S. Atomic Energy Commission and the National Science Foundation, Washington, D.C. 1970.
2. R. S. Lillard and D. P. Butt, *Preliminary Spallation Neutron Source Corrosion Experiments: Corrosion Rates of Engineering Materials in a Water Degrader Cooling Water Loop Irradiated by an 800 MeV Proton Beam*, Los Alamos National Laboratory Report, LAUR 96-1011, 1996.
3. L. B. Kriksunov, D. D. Macdonald, and P. J. Millett, *J. Electrochem. Soc*., **141** [11] 1994.
4. B. Soptrajanov, A. Nikolovski, and I. Petrov, *Spectrochimica Acta*, **24A**, 1617 (1968).
5. M. F. Daniel, B. Desbat, J.C. Lassegues, B. Gerand, and M. Figlarz, *J. Solid State Chem.*, **67**, 235 (1987).
6. D. S. Kim, M. Ostromecki, I. E. Wachs, S. D. Kohler, and J. G. Ekerdt, *Catalysis Lett*., **33**, 209 (1995).
7. M. Pourbaix, *Atlas of Electrochemical Equilibria*, pp 280-285, NACE, Houston, TX, 1974.